Molecular Structure and Adsorption of Dimethyl Sulfoxide at the Surface of Aqueous Solutions

H. C. Allen,† D. E. Gragson,‡ and G. L. Richmond*

Department of Chemistry, University of Oregon, Eugene, Oregon 97403

Received: April 28, 1998; In Final Form: November 20, 1998

Surface vibrational sum frequency generation (VSFG) spectroscopy complemented with surface tension measurements has been utilized to probe the air/ dimethyl sulfoxide (DMSO) interface as a function of DMSO concentration in water. For the neat DMSO surface, the DMSO methyl groups extend away from the liquid phase and VSFG polarization studies show that the methyl transition dipole moments of pure DMSO are on average oriented a maximum of 55° from the surface normal. A blue shift of the methyl symmetric stretch is observed with decreasing DMSO concentration and attributed to an electronic interaction between the sulfur and the methyl groups of DMSO. From surface tension data of the aqueous DMSO system, it is shown that DMSO number densities are higher at the surface of DMSO−water solutions relative to bulk DMSO concentrations revealing surface partitioning effects. Structural changes of surface DMSO are discussed in terms of monomers, dimers, and clusters which could account for the large differences in VSFG intensities and surface number densities. From surface tension measurements and utilizing DMSO activities, ΔG^0_{ads} is calculated to be −19.8 (±0.4) kJ/mol.

Introduction

The study of dimethyl sulfoxide (DMSO) adsorbed at a liquid surface has relevance to a broad range of topics in environmental and medicinal science. Understanding the surface adsorption and surface partitioning properties of DMSO is important since DMSO is an intermediate in the atmospheric oxidation of dimethyl sulfide (DMS).[1−5] DMSO is also important because of its utilization in a broad range of applications in medicine.[6] DMSO easily penetrates biological membranes, facilitates chemical tansport into biological tissue and is well-known for its cryoprotective effects on biological systems. [6−8] Also well established is the use of DMSO as an antiinflammatory agent which commonly has been used for arthritic conditions.[6] DMSO has also been utilized as an in situ free radical scavenger for various cancer treatments.[9] The unique properties of DMSO also give rise to its wide use as a solvent. Solvent properties of bulk DMSO have been exploited for several decades, and its applications span many areas of science.

Recently, the importance of studying aqueous DMSO surfaces has become more apparent. Oceanic DMS, the dominant source of atmospheric sulfur in the southern hemisphere,[10] oxidizes in the atmosphere to intermediates such as DMSO and eventually forms methanesulfonic acid (MSA) and sulfuric acid. Neither DMS oxidation mechanisms nor the role of DMSO in such processes is completely understood.[4] Atmospheric measurements of MSA have revealed that high MSA particle concentrations coexist with lower than expected MSA gas-phase concentrations.[11,12] In addition, the aqueous phase in-cloud oxidation of DMSO to form MSA is inferred from recent modeling studies in which DMSO appears to be the major source of MSA in the aerosol phase.[14] Dependent on relative humidity and aerosol number densities, atmospheric partitioning of DMSO from the gas phase to the aqueous phase is likely to occur due to its large Henry's law constant (9.9×10^4 mol kg^{-1} atm^{-1})[13] and mass accommodation coefficient of 0.10 (at 273 K).[2] Gas-phase adsorption of a species such as dimethyl sulfoxide is the first step before absorption into bulk solution.[15] Consequently, studying the properties of the air/DMSO−water interface and the surface partitioning of DMSO in water has relevancy.

In this study we examine the molecular structure of DMSO at the neat liquid DMSO surface and at the surface of aqueous solutions of varying bulk concentrations of DMSO. There have been very few studies exploring DMSO at a liquid surface in contrast to the many bulk liquid studies. Recently, Dabkowski et al.[16] and Karpovich and Ray[17] have investigated the surface of the aqueous DMSO system at low concentrations (<0.07 DMSO mole fraction) using surface tension and second harmonic generation (SHG), respectively. Their studies show evidence for surface partitioning of DMSO at an aqueous surface. The studies presented here are focused explicitly on examining DMSO at the solution surface by VSFG. Similar to SHG and surface tension measurements, VSFG is surface selective. However, VSFG also provides information about the molecular structure of an adsorbate which is inherent in any type of vibrational spectroscopy. The combination of this powerful surface specific spectroscopic technique[18−20] with surface tension measurements allows us to provide valuable information which may have important implications for chemistry at the surface of atmospheric aerosols and at interfaces of biological significance.

Much is known about the unique properties of DMSO in a bulk liquid. DMSO has a pyramidal structure with sulfur at the apex where the C−S−C bond angle is ∼ 96.4°, the O−S−C bond angle is ∼106.7°, C−S bond length is 1.8 Å, and S−O 1.5 Å. Two resonance structures can be drawn for DMSO where the S−O bond order is ∼1.5. The dipole moment is 4.11 D for

* To whom correspondence should be addressed.
† Postdoctoral fellow for the NOAA Postdoctoral Program in Climate and Global Change: UCAR Visiting Scientist Programs.
‡ Current address: Department of Chemistry and Biochemistry, California Polytechnic State University, San Luis Obispo, CA 93407.

10.1021/jp9820323 CCC: $18.00
Published on Web 01/08/1999

neat DMSO.[6] The high capacity of DMSO for solvating both polar and nonpolar molecules, in addition to DMSO dimer formation in solution, has been well documented.[6,21,22] The strong interactions between DMSO and water also disallow the convenience of assuming ideality of the aqueous solution. Therefore, activities rather than mole fractions should be used when interpreting raw data. The electron donating and accepting capacity by the sulfur and the oxygen give DMSO both its acid and basic characteristics. It has been termed as a supersolvent and has been documented as a rate accelerator for certain reactions.[6]

The affinity for DMSO to bond with itself has been reported for a number of bulk liquid systems. DMSO has been found to exist as chainlike aggregates in solution. It has also been postulated that at high DMSO concentrations an equilibrium exists between chainlike and ringlike aggregates.[6] Indicative of self-association characteristics, frequency shifts shown in spectroscopic studies are well documented for bulk DMSO−water systems.[6,23] In addition, DMSO molecules may form clusters which protect H_2O molecules from the hydrophobic DMSO methyl groups.[7] At high concentration in benzene, DMSO has been shown to form chain polymers. In 0.08−0.30 M DMSO in carbon tetrachloride solutions, DMSO forms dimers.[22] The S−O bond entity may be aligned with the O−S bond of an adjacent molecule (i.e., cyclic dimer), revealing strong self-association characteristics. DMSO self-association was studied in acetonitrile solutions from 0 to 14.04 DMSO mol L^{-1}. At DMSO concentrations approaching 5 mol L^{-1} in acetonitrile, spectroscopic studies show that 50% of the DMSO molecules are in the cyclic dimer formation relative to the monomer form.[21] The self-association properties may have relevance on the heterogeneous chemistry of DMSO at an interface.

VSFG Background. Surface vibrational sum frequency generation spectroscopy has been employed in this study to probe the surface of aqueous DMSO solutions. VSFG is a surface-specific nonlinear optical technique that has been used extensively in the study of surfaces and interfaces and which is sensitive to surface number density, orientation, and Raman and infrared transition probabilities. The theory has been well developed.[24−26,19] Therefore only a brief summary is given here.

The intensity, I_{sfg}, of the VSFG signal is proportional to the square of the surface nonlinear susceptibility $\chi_s^{(2)}$ which is a function of the sum frequency ($\omega_{sfg}=\omega_{vis}+\omega_{ir}$) generated from a noncentrosymmetric media.

$$I_{sfg} \propto |P_{sfg}|^2 \propto |\chi_{NR}^{(2)} + \sum_{\nu} |\chi_{R_\nu}^{(2)}| e^{i\delta_\nu}|^2 I_{vis} I_{ir} \qquad (1)$$

P_{sfg} is the nonlinear second-order polarization, δ_ν is the phase factor, and I_{vis} and I_{ir} are the intensities for the incident visible and infrared beams. The resonant term $\chi_{R_\nu}^{(2)}$ dominates when the infrared frequency is resonant with a vibrational mode of a molecule at the surface or interface and is proportional to the number density of orientationally averaged molecules. Whereas the nonresonant term $\chi_{NR}^{(2)}$ is negligible. The surface susceptibility is a 27 element tensor and can be reduced to a few nonvanishing elements by invoking symmetry constraints. Assuming an isotropic surface in the surface plane, $\chi_s^{(2)}$ reduces to four independent nonzero elements

$$\chi_{zzz}^{(2)}, \quad \chi_{xxz}^{(2)} = \chi_{yyz}^{(2)}, \quad \chi_{xzx}^{(2)} = \chi_{yzy}^{(2)}, \quad \chi_{zxx}^{(2)} = \chi_{zyy}^{(2)} \qquad (2)$$

where z is defined as normal to the surface. These four nonreducible elements contribute to the VSFG intensity. The first two polarization combinations of the four shown below were used in the DMSO studies presented.

$$I_{ssp} \propto |F_i f_i f_z \chi_{iiz}^{(2)}|^2 \qquad (3a)$$

$$I_{sps} \propto |F_i f_z f_i \chi_{izi}^{(2)}|^2 \qquad (3b)$$

$$I_{pss} \propto |F_z f_i f_i \chi_{zii}^{(2)}|^2 \qquad (3c)$$

$$I_{ppp} \propto |F_i f_i f_z \chi_{iiz}^{(2)} + F_i f_z f_i \chi_{izi}^{(2)} + F_z f_i f_i \chi_{zii}^{(2)} + F_z f_z f_z \chi_{zzz}^{(2)}|^2 \qquad (3d)$$

The subscripts ssp on the intensity ***I*** denote the sum, visible, and infrared polarizations, respectively. The subscript ***i*** denotes the ***x*** or ***y*** polarizations and the ***F*** and ***f*** are the Fresnel coefficients for the reflected and incident waves, respectively. In order for a surface to be sum frequency active, the vibrational modes must be both Raman and IR active. The different polarization combinations are sensitive to the direction of the IR and Raman transition moments, where the ppp polarization combination records all components of the resonant vibrational mode.

To estimate the orientations of the neat DMSO CH_3 group dipole transition moments at the air/DMSO interface, the approach presented by Eisenthal and co-workers[27] was employed. The final equation from which orientation is determined is

$$\theta = \text{arc cot}\left[\left(\frac{\chi_{xxz}^{(2)}}{\chi_{xzx}^{(2)}} - \frac{1+R}{1-R}\right)\frac{1-R}{2R}\right]^{1/2} \qquad (4)$$

where θ is assumed to have a delta function distribution and is an average angle of all azimuthal angles of the CH_3 transition dipole moment relative to the surface. Physically, θ represents the angle between the C_{3v} axes of the CH_3 groups and the surface normal. R is the molecular hyperpolarizability ratio. The ratio of $\chi_{xxz}^{(2)}$ to $\chi_{xzx}^{(2)}$ is rearranged using eqs 3a and 3b and is shown in eq 5. From previous sum frequency experiments on the deuterated methyl group of $CD_3(CH_2)_{19}CN$, this ratio which determines the phase of the hydrophobic methyl group, was experimentally found to be negative.[27]

$$\frac{\chi_{xxz}^{(2)}}{\chi_{xzx}^{(2)}} = \frac{F_s f_p f_s}{F_s f_s f_p}\sqrt{\frac{I_{ssp}}{I_{sps}}} \qquad (5)$$

The Fresnel coefficients for each of the three fields are calculated utilizing the angles of the reflected and incident laser beams. In addition, R from eq 4 can be simplified from the molecular hyperpolarizability ratio to being related to the Raman depolarization. If the transition is completely symmetric this ratio is defined as

$$R = \left(\frac{Q-1}{Q+2}\right) \qquad Q = \left[\frac{3}{5}\left(\frac{1}{\delta} - \frac{4}{3}\right)\right]^{1/2} \qquad (6)$$

where δ is the Raman depolarization ratio. The value of $\delta = 0.03$ from DMSO Raman studies completed by Forel and Tranquille[28] was used for these calculations.

Experimental Section

The laser system utilized for these VSFG studies consists of a Ti:sapphire regenerative amplifier system that pumps a two-stage optical parametric amplifier (OPA). The two stage amplifier is also seeded with a portion (1−1.6 μm) of white

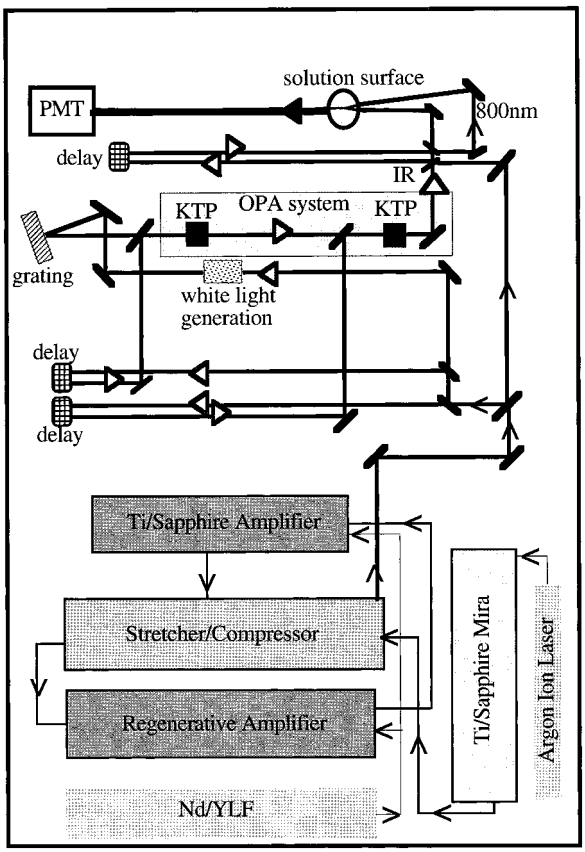

Figure 1. Surface vibrational sum frequency laser setup utilized for DMSO spectroscopy experiments. Two laser beams (800 nm and 2.4−4.0 μm infrared) are overlapped on the DMSO−water surface, and the reflected nonlinear sum frequency is detected by a photomultiplier tube (or CCD camera) after spatial, temporal, and frequency filtering.

light continuum generated from pumping ethylene glycol with a portion of the 800 nm beam. The VSFG laser system has been described in detail elsewhere.[29] Some of the DMSO VSFG spectra were obtained after the Ti:sapphire regenerative amplifier had been upgraded to incorporate a second Ti:sapphire amplifier system. This upgrade has more than doubled the available laser power in both the 800 nm beam and the infrared beam. The system produces 1.9 ps pulses at a repetition rate of 1 kHz. Most spectra were obtained under S_{sfg} S_{vis} P_{ir} polarization conditions which couples with the vibrational mode components that are perpendicular to the plane of the interface. S_{sfg} P_{vis} S_{ir} polarization studies were also completed to identify the surface bond orientations. A diagram of the VSFG system is shown in Figure 1.

Two collinear laser beams generated from the same laser system, 800 nm and tunable infrared (2.4−4.0 μm), are overlapped at the air/DMSO−water interface. The sum of the two frequencies is produced at the interface. Thus, the reflected 800 nm, reflected infrared beam, and the sum frequency beam propagate away from the interface in a defined direction. The three beams are separated spatially according to momentum conservation requirements and the sum frequency signal is detected with a photomultiplier detector (or CCD camera) after further filtering. To obtain a vibrational spectrum, the tunable infrared beam is scanned over the 2.4−4.0 μm range, and the signal detected is coordinated in time with the infrared wavelength produced in the two stage amplifier by angle tuning of the nonlinear crystals (KTP). The wavelength calibration is completed by peak wavelength comparison from a pentadecanoic acid monolayer standard and use of a monochromator.

TABLE 1: DMSO Mole Fractions, Activities, Weight Fractions, and Molarities

DMSO mole fraction	DMSO activity	DMSO weight fraction	DMSO molarity
0.015	0.001	0.06	0.8
0.044	0.003	0.17	2.1
0.060	0.005	0.22	2.8
0.090	0.009	0.30	4.0
0.15	0.02	0.43	5.8
0.20	0.04	0.52	7.0
0.34	0.16	0.69	9.4
0.42	0.26	0.76	10.4
0.50	0.37	0.81	11.3
0.63	0.56	0.88	12.3
0.71	0.67	0.91	12.8
0.83	0.82	0.95	13.4
0.91	0.90	0.98	13.7
1.0	1.0	1.0	

Spectral bandwidth for this system is 17 cm^{-1} fwhm. Data points were obtained every 0.001 μm ($\sim$1 cm^{-1}). For the DMSO experiments, the laser spot size diameter for the 800 nm beam was $\sim$1 mm and $\sim$0.3 mm for the infrared beam, and the beam energies were typically 200 and 6 μJ, respectively. At the interface, the infrared beam was focused at the sample surface using a 15 cm focal length lens. To avoid solution perturbation in the high DMSO concentration regime, the 800 nm beam was focused 3.5 cm before the sample using a 55 cm focal length lens. Saturation of the surface oscillators was avoided by lowering the incident beam intensities to check that the VSFG signal intensity for the vibrational modes to be studied also decreased accordingly. Between spectra acquisitions of varying DMSO concentration, VSFG spectra of pure DMSO were acquired. These spectra were used as an additional calibration to monitor variations in laser intensity. Spectral peaks were fit using a combination of Gaussian−Lorentzian functions. VSFG spectra were typically acquired at 22 ($\pm$2) °C.

The Wilhelmy plate method was utilized to measure the surface tension of the DMSO and water solutions. The Wilhelmy plate is a carefully sandblasted platinum plate which is partially placed in the aqueous solution at the air/liquid interface. The surface tension is dependent on the downward force that is exerted by the plate and is measured using an electrobalance (KSV Instruments). Free energy of adsorption was calculated utilizing the Gibbs equation followed by employment of Langmuir isotherm equations for both the surface tension and VSFG data. All VSFG and surface tension measurements (21 °C), were obtained from containers open to the atmosphere. The excellent agreement for the surface tension measurements with other published data[30] indicate that the surface environment is not significantly sensitive to an open versus closed (in equilibrium) system for aqueous DMSO solutions. Dimethyl sulfoxide, chemical purity 99.9%, was obtained from Aldrich. HPLC water was obtained from Mallinckrodt.

Results and Discussion

Nonideality of the aqueous DMSO solutions results in large discrepancies between mole fractions and the corresponding calculated activities, particularly at low solute concentrations.[7,31,32] Therefore in the data interpretation to follow, both activities and mole fractions are employed. DMSO mole fractions, weight fractions, molarities, and the corresponding activities[7,31] are shown in Table 1. Weight fractions and molarities are given for ease of comparison with other published results.

Figure 2 shows sum frequency vibrational spectra (ssp polarizations) of DMSO at the air/liquid interface at different

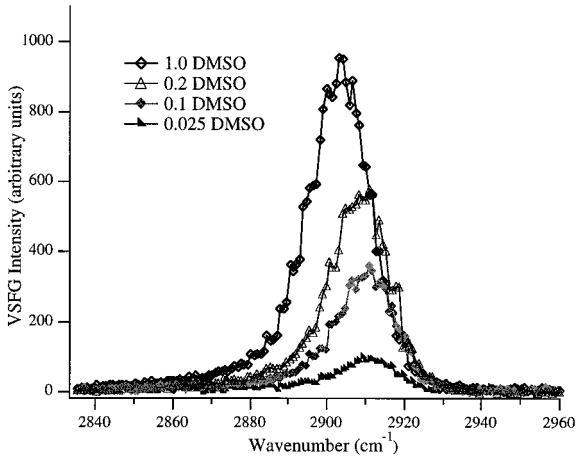

Figure 2. VSFG spectra show the CH_3-SS and the CH_3 overtone modes of DMSO as a function of DMSO mole fraction.

mole fractions of DMSO in the bulk solution. In the spectrum of the neat DMSO surface, the peak at 2903 (± 0.5) cm^{-1} (blue shifted to 2910 (± 0.5) cm^{-1} at lower mole fractions) is assigned to the CH_3 symmetric stretch (CH_3-SS). The VSFG CH_3-SS peak dominates the spectrum in the range of 2750 to 3150 cm^{-1}. The shoulder at 2890 cm^{-1} and the tail to the red of the shoulder are assigned to overtones of the degenerate CH_3 deformation modes of DMSO which exist in the 1400−1450 cm^{-1} region.[33] One might attribute the asymmetry on the high energy side of the CH_3-SS to an additional weak mode, but further studies are necessary to verify this. The CH_3-SS peak is shown to decrease in intensity with decreasing DMSO concentrations. In addition to the change in VSFG intensity with decreasing DMSO concentration, there is a blue shift of the CH_3-SS from 2903 to 2910 (± 0.5) cm^{-1}. The spectra in Figure 2 are the first VSFG studies for surface DMSO from neat and aqueous DMSO solutions to be published.

Our studies show that the CH_3-SS of DMSO at the neat DMSO surface occurs at 2903 cm^{-1} and is significantly red shifted from this mode examined in bulk Raman and infrared DMSO studies. Previous studies of bulk liquid DMSO show the DMSO methyl symmetric stretch at 2914[28] and 2915 cm^{-1} [33] (infrared and Raman, respectively), and gas-phase infrared studies show the CH_3-SS at 2908 cm^{-1}.[28] We attribute this shift to an increased interaction between the lone pair of electrons from the sulfur and the CH bonds from the methyl groups which can result in a significant red shift as shown from previous bulk studies of oxygen, nitrogen, and sulfur linkages to methyl groups.[34−37] Crowding of the hydrophobic methyl groups of neat DMSO at the surface may help to stabilize these electronic effects leading to the observed red shift from the CH_3-SS for surface DMSO relative to what is found from bulk DMSO Raman and IR studies.

An orientation study of the methyl groups symmetry axes of DMSO relative to the surface normal for pure DMSO at the neat air/DMSO interface was completed by employing the methods discussed above (eqs 4−6) and utilizing both ssp and sps polarization spectra results. For pure DMSO solutions, a methyl group maximum tilt angle of 55° from the surface normal was determined from VSFG spectral peak intensities and should be taken as an upper limit due to error propagation from the background intensity levels. Weak signal intensities from sps spectroscopy studies are typical,[38] and for the DMSO studies, the CH_3-SS sps signal intensities were below our background signal levels, resulting in the indicated large uncertainty in the angle measurement. Nevertheless, the ratio of $\boldsymbol{I}_{ssp}$ to $\boldsymbol{I}_{sps}$ allowed a maximum tilt angle to be calculated.

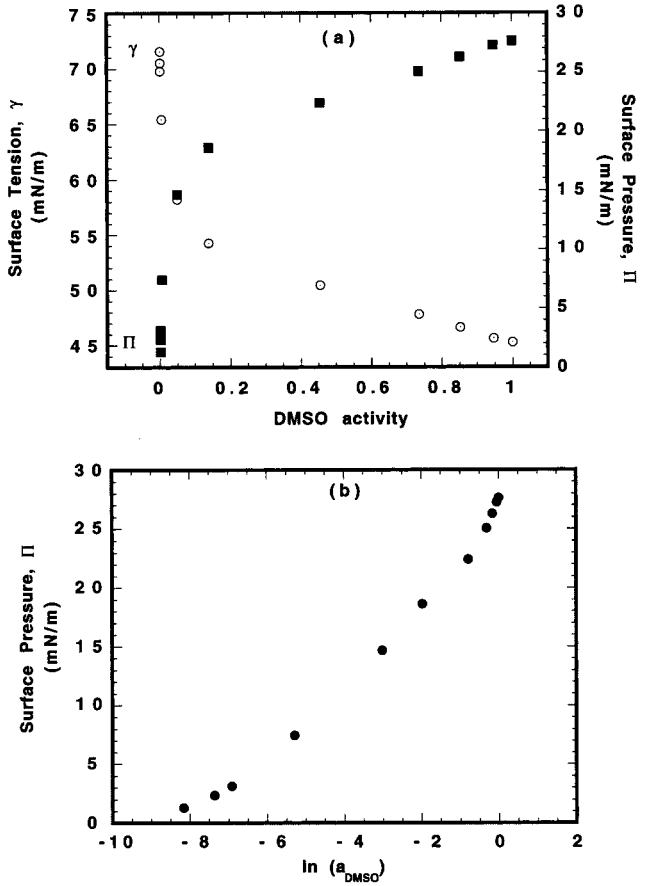

Figure 3. (a) DMSO surface tension (γ) and pressure (Π) measurements. (b) A plot of DMSO surface pressure versus the natural logarithm of the DMSO activity.

To analyze the amount of DMSO at the surface, surface tension measurements were conducted and the results are shown in Figure 3a. The surface tension γ of pure DMSO is 45 mN/m and that of pure water is 73 mN/m. All measurements obtained agree well with previously published surface tension data over the full concentration range.[6,30] In addition, Figure 3a shows the surface pressure measurements Π (surface tension of pure water minus the surface tension of the solution measured) as a function of DMSO activity. Figure 3b is a plot of surface pressure Π versus the natural logarithm of DMSO activity. By utilizing the Gibbs equation, the derivative of the surface pressure with respect to the change in the natural logarithm of the DMSO activity is derived and the resulting DMSO surface excess Γ is calculated from eq 7

$$\Gamma = \frac{1}{kT}\left(\frac{\mathrm{d}\Pi}{\mathrm{d}\ln a_{\mathrm{DMSO}}}\right)_T \tag{7}$$

where Π is the surface pressure, k is the Boltzmann constant, T is the temperature, and a_{DMSO} is the DMSO activity.[39] Figure 4 shows the surface excess as a function of activity. Figure 5 shows a plot of the surface area occupied per DMSO molecule which is the reciprocal of the surface excess Γ added to the two-dimensional bulk number density versus DMSO activity. The surface area calculation is shown in eq 8.

$$\text{DMSO surface area} = \frac{1}{\Gamma + X_{\mathrm{DMSO}}(\rho_{\mathrm{DMSO}})^{2/3}} \tag{8}$$

The DMSO surface area is the area occupied by a DMSO molecule on the solution surface, X_{DMSO} is the DMSO mole

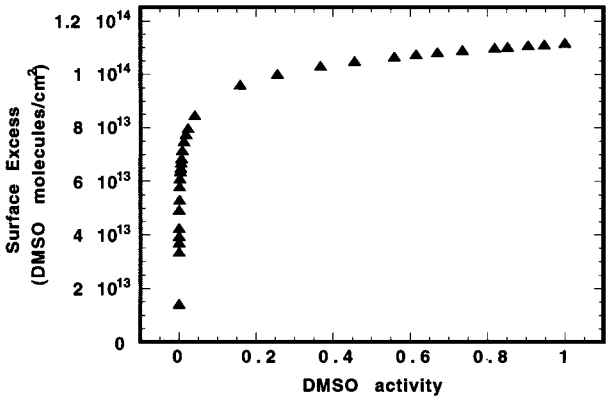

Figure 4. DMSO surface excess Γ as a function of DMSO activities.

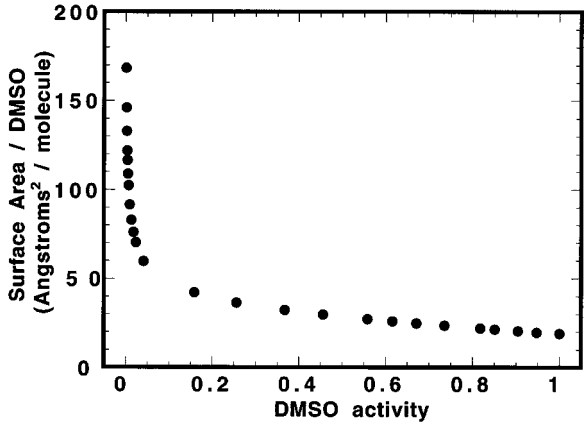

Figure 5. Surface area occupied by DMSO as a function of DMSO activity.

fraction, and ρ_{DMSO} is the bulk density of DMSO (after partial molar volume corrections). At DMSO surface saturation, each DMSO entity occupies a surface area of 19 Å^2 which corresponds to 5.3×10^{14} molecules cm^{-2}. Our results agree reasonably well with the projected area of 24 Å^2 derived from DMSO molecular volumes.[16] Since the methyl groups extend out of the liquid phase rather than the sulfur, one would expect the area per DMSO to be smaller than the projected area in which sulfur is at the apex of the pyramidal structure. In addition, crowding at the surface, as is suggested by the observed spectral shifts, may account for smaller surface areas occupied per DMSO molecule at the neat air/liquid interface. The surface area occupied by DMSO gradually increases, and in the limit of low concentration (<0.15 activity), a steep increase in area occupied by DMSO is observed. A relatively constant surface area of 40 Å^2 to 19 Å^2 is observed from 0.15 to 1.0 DMSO activity. This relatively constant surface area indicates that surface partitioning and self-association of DMSO may be significant factors affecting the surface structure of DMSO at the air/liquid interface.

For DMSO, one might expect that the surface concentration would be mirrored by the bulk concentration. However, this is clearly not the case as surface partitioning is occurring to a large extent throughout the concentration range examined here as shown in the surface excess (Figure 4) and the surface area (Figure 5) plots. Even at low concentrations there exists a large surface excess compared to the bulk concentration as shown in the surface excess studies consistent with recent studies conducted by Dabkowski et al.[16] and Karpovich and Ray.[17]

Interesting trends are also observed in the spectroscopic measurements conducted at different DMSO concentrations. In

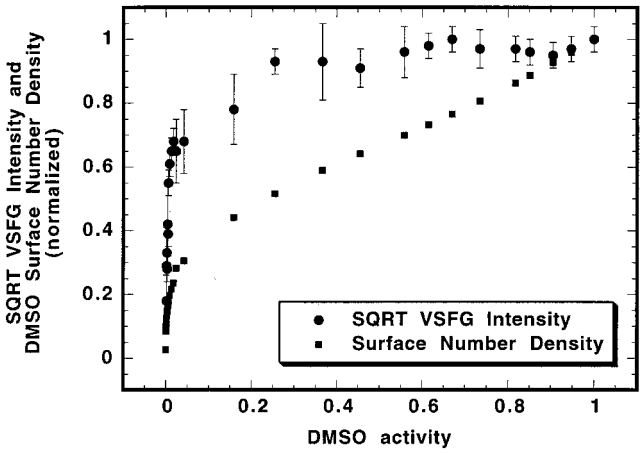

Figure 6. This plot shows the normalized square root of the VSFG CH_3-SS intensity of DMSO and the total DMSO surface number density (derived from surface tension measurements) versus bulk DMSO activities.

interpreting such trends it is important to note that several factors can influence the observed intensity. Since the SFG response is proportional to the square root of the number density, a change in the number density of molecules or contributing oscillators at the solution surface will alter the observed VSFG intensity. Second, since we are probing the surface with infrared that is polarized perpendicular to the surface, a change in the molecular orientation along the surface normal will be reflected in the intensity.

Figure 6 shows a plot of the square root of the integrated VSFG intensity measured from the methyl peak areas as a function of bulk DMSO activities. Intensities were derived from curve fits to the spectra. The square root of the integrated peak areas are normalized to a DMSO activity of 1.0. The data shows a sharp rise in surface VSFG intensity as the DMSO bulk concentration increases. At approximately 0.2 DMSO activity ($X_{DMSO} \approx 0.4$), the VSFG intensity plateaus, and from 0.3 to 1.0 activity the integrated intensity is relatively constant. Also shown in Figure 6 are the DMSO surface number densities (denominator in eq 8) derived from the surface tension data and bulk number density.

A comparison of the VSFG and the surface tension data both shown in Figure 6 reveals that the square root of the VSFG intensity does not track with the surface number density. We attribute the larger increase in VSFG intensity relative to the surface density to a reorientation of surface DMSO as the surface concentration increases as discussed more below.

Accompanying this large increase in intensity with surface concentration is a corresponding shift in methyl stretching frequency. Referring to Figures 2 and 7, the VSFG data shows that the methyl symmetric stretch gradually blue shifts from 2903 to 2910 cm^{-1} with decreasing concentration. We attribute this shift to a decrease in the electronic interaction between the sulfur and the methyl group as the surface concentration of DMSO molecules decreases. The frequency shift is indicative of changing intermolecular interactions involving DMSO self-association and DMSO association with water. With decreasing DMSO concentrations, the reduced crowding at the surface and increased DMSO−water interaction may help to destabilize the sulfur and methyl electronic interaction thereby allowing a gradual blue shift to occur. It is interesting that the CH_3-SS frequency at the lowest concentration as measured here blue shift in the direction toward the 2908 cm^{-1} gas phase and the 2915−2914 cm^{-1} bulk neat liquid measurements for this mode by infrared and Raman.

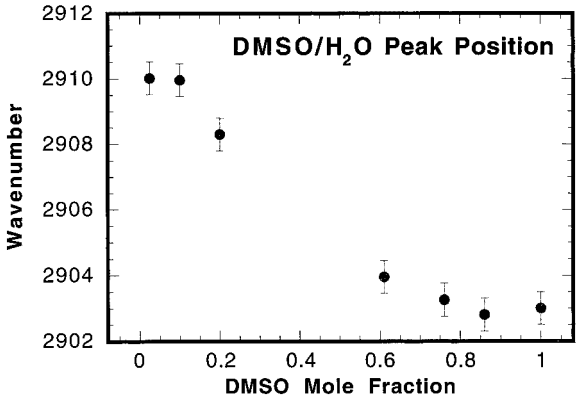

Figure 7. The peak position of the surface DMSO CH_3-SS as a function of DMSO mole fraction.

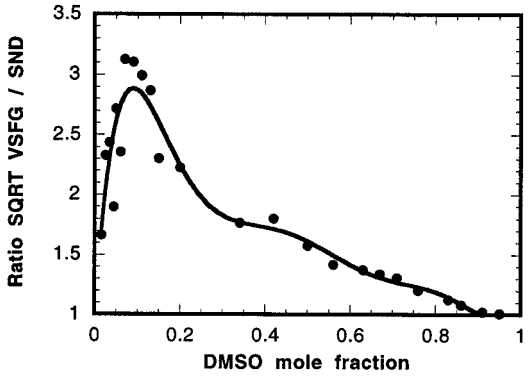

Figure 8. The calculated ratio of the square root of the DMSO VSFG CH_3-SS intensity to the DMSO surface number density (the curve fit is a guide to the eye) versus bulk DMSO mole fraction.

Similar to the CH_3-SS blue shift that we observe with decreasing concentration, Forel and Tranquille[28] also observed a CH_3-SS blue shift with decreasing DMSO concentration in carbon tetrachloride solutions utilizing infrared spectroscopy. Previously, the vibrational frequency for the S−O stretching mode of DMSO was shown to shift from 1046 to 1013 cm^{-1} (Δ33 cm^{-1} red shift) from neat DMSO to dilute DMSO−water solutions respectively, due to solvent effects.[6] In addition, red shifts from Raman spectra have been recorded by Scherer et al.[23] for ν_b, ν_d, and the ν_w (OH bonded, H_2O dibonded, OH weakly bonded, respectively) modes of H_2O going from DMSO-rich solutions to dilute DMSO in water solutions.

An important factor in understanding the intermolecular interactions of DMSO at the surface is the fact that DMSO has a strong affinity for self-association. Also well established is the nonideal behavior of DMSO in aqueous solutions. Strong interactions of DMSO with water is suggestive of cluster aggregation of DMSO in aqueous solutions where the hydrophobic methyl groups protect themselves from the polar water molecules. This type of association at high DMSO bulk concentrations has been postulated from thermodynamic studies.[7] Such self-association could be playing a significant role in the observed change in DMSO orientation with concentration.

To shed further light on the changing environment of surface DMSO as a function of surface concentration, Figure 8 is a plot of the ratio of the VSFG intensity and the surface number density as a function of bulk DMSO mole fraction. The largest changes in this ratio are observed at low concentrations below $X_{DMSO} = 0.15$ which we attribute to reorientation of the methyl group toward a more perpendicular orientation with the surface normal. This is also the concentration region where the largest change in DMSO surface area is occurring (see Figure 5). Beyond $X_{DMSO} = 0.15$ an abrupt change in the ratio is observed with the ratio declining rapidly up to $X_{DMSO} = 0.20$ and more gradually beyond. There are several factors that could be responsible for this abrupt change in surface DMSO structure and orientation with concentration, the most likely being aggregation of DMSO molecules at the surface. Such aggregation to form dimers or higher order clusters is also consistent with the large surface number density found in the surface tension data at these concentrations. The large surface number density is then accounted for from the DMSO aggregates that might contribute minimally to the net VSFG signal intensity due to cancelation of the opposing orientations of the methyl groups relative to the surface normal. Consistent with this picture, a complex surface mixture of DMSO monomers and aggregates exists which may be influenced by surface steric effects and competing attractions between DMSO with itself and with water. The observed asymmetry of the CH_3-SS peak shown in Figure 2 could be attributed to surface monomers as mentioned above. The observed shift away from this possible mode with increasing DMSO concentration is suggestive of a molecular environment in which DMSO may aggregate which is consistent with a decrease in the ratio shown in Figure 8 at DMSO concentrations higher than 0.15 mole fraction. Additional VSFG and possibly SHG studies are warranted to help deconvolute and identify the complex mixtures of surface DMSO aggregates as a function of concentration.

From the surface number calculations from surface tension data at low DMSO activities (<0.006) and utilizing Langmuir isotherm equations, the free energy of adsorption ΔG^0_{ads} is calculated to be −19.8 (± 0.4) kJ/mol. If one uses VSFG measurements as a means of measuring ΔG^0_{ads}, a value of −15 kJ/mol is obtained. However, as noted above, the VSFG intensity measurements at lower concentrations could be complicated by adsorbate orientation effects.

Previous studies have utilized mole fractions when calculating thermodynamic parameters such as ΔG^0_{ads} for DMSO aqueous solutions. For an ideal solution this is appropriate. However, as discussed above, DMSO and water interact strongly and mixtures form nonideal solutions particularly in the low concentration regime. Therefore it is more appropriate to utilize DMSO activities. For comparison to other published data, we have also calculated the ΔG^0_{ads} for DMSO aqueous solutions using mole fractions from surface tension data rather than activities. This revealed a smaller absolute value for the free energy of adsorption, −13 kJ/mol. Also utilizing DMSO mole fractions and surface tension data, Dabkowski et al.[16] and Karpovich and Ray [17] published a ΔG^0_{ads} of −9.8 and −11.8 (σ = 1.2) kJ/mol, respectively, for the DMSO−water system. Due to nonideality of the DMSO−water system, utilizing DMSO activities and surface tension data, we believe a more accurate ΔG^0_{ads} for DMSO based on activities is −19.8 (± 0.4) kJ/mol.

The Langmuir isotherm equation utilized for the free energy of adsorption calculations is shown below.[39]

$$\Theta_{DMSO} = \frac{\frac{m}{b} a_{DMSO}{}^{b}}{\frac{m}{b} a_{DMSO}{}^{b} + 1}; \quad \frac{m}{b} = K = \frac{a_{DMSO}{}^{s}\, a_{water}{}^{b}}{a_{water}{}^{s}\, a_{DMSO}{}^{b}} \qquad (9a,b)$$

Θ_{DMSO} is the fractional surface coverage of DMSO, K is the equilibrium constant for DMSO adsorption in competition with water to the surface from the bulk, and a^s and a^b are the activities for the surface and the bulk, respectively. By fitting a line with

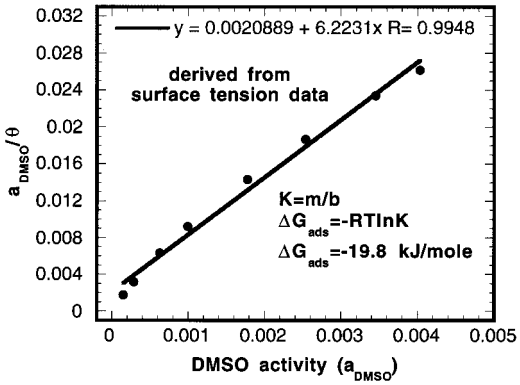

Figure 9. This plot shows the DMSO activity divided by the DMSO surface coverage as a function of DMSO activity. The DMSO free energy of adsorption is calculated.

slope m and y-intercept b to eq 10, K is found.[39]

$$\frac{a_{\mathrm{DMSO}}{}^{b}}{\Theta_{\mathrm{DMSO}}} = m a_{\mathrm{DMSO}}{}^{b} + b \tag{10}$$

The equilibrium constant K is related to $\Delta G^0_{\mathrm{ads}}$ by eq 11.

$$\Delta G^0_{\mathrm{ads}} = -RT \ln K \tag{11}$$

Figure 9 shows the fit (R coefficient better than 0.99) to the surface excess data from which the equilibrium constant K is derived and $\Delta G^0_{\mathrm{ads}}$ is calculated.

Conclusions

The vibrational spectroscopy of DMSO at a liquid surface has been reported here for the first time using VSFG. In the spectral region examined, the methyl symmetric stretch of DMSO at the surface of the pure DMSO solution is red shifted relative to bulk liquid and gas-phase Raman and infrared studies which is likely due to an increase in the electronic interaction of the lone pair from the sulfur with the methyl groups of the DMSO and is stabilized by surface crowding effects. The DMSO methyl symmetric stretch from surface DMSO gradually blue shifts with decreasing DMSO concentration. The blue shift may be correlated with a destabilization of the sulfur−CH electronic interaction with decreasing surface concentration.

The surface partitioning of DMSO in water observed from surface tension data is clearly occurring over all concentration ranges. DMSO surface partitioning effects give rise to free energies of adsorption of −19.8 (± 0.4) kJ/mol. In the low concentration regime, we conclude that DMSO monomers dominate as the preferred surface structure. The noncoincidence between the VSFG results and surface number densities at higher concentrations is suggestive of self-association of DMSO molecules at the surface, possibly a mixture of dimers and clusters of DMSO in addition to DMSO monomers. In the low concentration regime, DMSO surface partitioning may have implications for chemical reactivity of DMSO at the air/DMSO−water interface with respect to surface chemistry of atmospheric aerosols. Future orientation studies and water studies are planned in the low concentration regime. In the high DMSO concentration regime, surface saturation of DMSO is clearly evident above 0.15 DMSO mole fraction which is particularly relevant to applications of solvation and biological membrane transport.

From our preliminary DMSO orientation work, the methyl transition dipole moments of neat DMSO are oriented a maximum of 55° from the surface normal. A thorough orientation study over the full DMSO concentration range at the air/liquid interface is planned in the future to help elucidate the complex DMSO structural changes that are inferred from the VSFG studies presented here.

Acknowledgment. The authors thank the NOAA Postdoctoral Program in Climate and Global Change and the Department of Energy (Grant DE-FG03-96ER45557) for the support of this work. We are also grateful to Professor Gil Nathanson, Dr. Bruce Chase, Dr. Gao Chen, Professor Jean Pemberton, and Dr. Anne Jefferson for helpful discussions.

References and Notes

(1) Capaldo, K. P.; Pandis, S. N. *J. Geophys. Res.* **1997**, *102*, 23251.
(2) DeBruyn, W. J.; Shorter, J. A.; Davidovits, P.; Worsnop, D. R.; Zahniser, M. S.; Kolb, C. E. *J. Geophys. Res.* **1994**, *99*, 16927.
(3) Davis, D.; Chen, G.; Kasibhatla, P.; Jefferson, A.; Tanner, D.; Eisele, F.; Lenschow, D. Neff, W.; Berresheim, H. *J. Geophys. Res.* **1998**, *103*, 1657.
(4) Hynes, A. J.; Wine, P. H. *J. Atmos. Chem.* **1996**, *24*, 23.
(5) Sorensen, S.; Falbe-Hansen, H.; Mangoni, M.; Hjorth, J.; Jensen, N. R. *J. Atmos. Chem.* **1996**, *24*, 299.
(6) Jacob, S. W.; Rosenbaum, E. E.; Wood, D. C. *Dimethyl Sulfoxide*; Marcel Dekker: New York, 1971; Vol. 1.
(7) Lai, J. T.; Lau, F. W.; Robb, D.; Westh, P. Nielsen, G.; Trandum, C.; Hvidt, A.; Koga, Y. *J. Sol. Chem.*, **1995**, *24*, 89.
(8) Scaduto, R. C. *Free Radical Biol. Med.* **1995**, *18*, 271.
(9) Salim, A. *Oncology* **1992**, *49*, 58.
(10) Barone, S. B.; Turnipseed, A. A.; Ravishankara, A. R. *Faraday Discuss.* **1995**, *100*, 39.
(11) Jefferson, A.; Tanner, D. J.; Eisele, F. L.; Davis, D. D.; Chen, G.; Crawford, J.; Huey, J. W.; Torres, A. L.; Berresheim, H. *J. Geophys. Res.* **1998**, *103*, 1647.
(12) Eisele, F.; Mauldin, L.; Tanner, D.; Jefferson, A. *Eos Suppl., Trans., AGU* **1997**, *78* (46), A41D-4.
(13) Watts, S. F.; Brimblecombe, P. *Environ. Technol. Lett.* **1987**, *8*, 483.
(14) Chen, G.; Davis, D. D.; Eisele, F. L.; Mauldin, L., Tanner, D. J.; Bandy, A. R.; Thornton, D. C.; Huebert, B. A42C-1, *Eos Suppl., Trans., AGU* **1997**, *78* (46), A42C-1.
(15) Davidovits, P.; Jayne, J. T.; Duan, S. X.; Worsnop, D. R.; Zahniser, M. S.; Kolb, C. E. *J. Phys. Chem.* **1991**, *95*, 6337.
(16) Dabkowski, J.; Zagorska, I.; Dabkowska, M.; Koczorowski, Z.; Trasatti, S. *J. Chem. Soc., Faraday Trans.*, **1996**, *92*, 3873.
(17) Karpovich, D. S.; Ray, D. *J. Phys. Chem. B*, **1998**, *102*, 649.
(18) Hunt, J. H.; Guyot-Sionnest, P.; Shen, Y. R. *Chem. Phys. Lett.* **1987**, *133*, 189.
(19) Bain, C. D. *J. Chem. Soc., Faraday Trans.* **1995**, *91*, 1281.
(20) Conboy, J. C.; Messmer, M. C.; Richmond, G. L. *J. Phys. Chem.* **1996**, *100*, 7617.
(21) Fawcett, W. R.; Kloss, A. A. *J. Chem. Soc., Faraday Trans.*, **1996**, *92*, 3333.
(22) Figueroa, R. H.; Roig, E.; Szmant, H. H. *Spectrochim. Acta* **1966**, *22*, 587.
(23) Scherer, J. R.; Go, M. K.; Kint, S. *J. Phys. Chem.* **1973**, *77*, 2108.
(24) Shen, Y. R. *The Principles of Nonlinear Optics*; John Wiley & Sons: New York, 1984.
(25) Dick, B.; Gierulski, A.; Marowsky *Appl. Phys. B* **1985**, *38*, 107.
(26) Dick, B. *Chem. Phys.* **1985**, *96*, 199.
(27) Zhang, D.; Gutow, J.; Eisenthal, K. B. *J. Phys. Chem.* **1994**, *98*, 13729.
(28) Forel, M.-T.; Tranquille, M. *Spectrochim. Acta* **1970**, *26A*, 1023.
(29) Gragson, D. E.; McCarty, B. M.; Richmond, G. L.; Alavi, D. S. *J. Opt. Soc. Am. B* **1996**, *13*, 2075.
(30) Cheong, W. J.; Carr, P. W. *J. Liq. Chromatogr.* **1987**, *10*, 561.
(31) Luzar, A. *J. Chem. Phys.* **1989**, *91*, 3603.
(32) Qian, X.; Han, B.; Liu, Y.; Yan, H.; Liu, R. *J. Solution Chem.* **1995**, *24*, 1183.
(33) Horrocks, W. D.; Cotton, F. A. *Spectrochim. Acta* **1961**, *17*, 134.
(34) Bellamy, L. J. *The Infrared Spectra of Complex Molecules*; John Wiley & Sons: New York, 1975.
(35) Higuchi, S.; Kuno, E.; Tanaka, S.; Kamada, H. *Spectrochim. Acta* **1972**, *28A*, 1335.
(36) McKean, D. C.; Duncan J. L.; Batt, L. *Spectrochim. Acta*, **1973**, *29A*, 1037.
(37) Krueger, P. J.; Jan, J. *Can. J. Chem.* **1970**, *48*, 3236.
(38) Bell, G. R.; Bain, C. D.; Ward, R. N. *J. Chem. Soc., Faraday Trans.* **1996**, *92*, 515.
(39) Hiemenz, P. C.; Rajagopalan, R. *Principles of Colloid and Surface Chemistry*, 3rd ed.; Marcel Dekker: New York, 1997.